Development of two types of high temperature calorimeters

Tsuneo Matsui[*], Yuji Arita, Kunihiro Watanabe

*Department of Quantum Engineering, Graduate School of Engineering, Nagoya University,
Furo-cho, Chikusa-ku, Nagoya 464-8603, Japan*

Abstract

For heat capacity measurement of ceramic materials at high temperatures above 1500 K, two new calorimeters, i.e. a high speed cooling calorimeter and an advanced-direct heating pulse calorimeter, have been developed in our laboratory. The high speed cooling calorimeter is assembled of an induction heating furnace, a paraboloidal mirror and a high speed six-wavelength pyrometer. In this calorimeter, the heat capacity is determined from the cooling rate of a sample dropped from the induction heating furnace. As a simulation of a dropped specimen, two different experiments on transient modes were made using a calibrated tungsten lamp in the temperature range 2060–2180 K: (1) by changing temperature with time (cooling curve measurement), and (2) by changing the position of a tungsten lamp vertically at constant temperature. Both results show reliability of this calorimeter at high temperatures. The advanced direct heating pulse calorimeter is a re-designed and re-constructed apparatus of the direct heating pulse calorimeter previously developed in our laboratory to increase the measuring temperature for the heat capacity up to 2000 K. By the improvement of a new vacuum vessel, molybdenum thermal insulator and tantalum heating wire, heat capacity and electrical conductivity of graphite could be measured up to 1750 K. © 2000 Elsevier Science B.V. All rights reserved.

1. Introduction

The heat capacity of energy-related materials at high temperatures is essentially important to predict and understand the thermophysical behavior, especially the behavior of nuclear fuels under normal and abnormal operational conditions of nuclear reactors. The heat capacity of UO_2 at high temperatures is one of the most important properties of the fuel materials. Several investigators revealed a pronounced increase in the heat capacity of UO_2 at temperatures above around 1600 K, the origin of which has been discussed for many years. Some representative results for heat capacity of UO_2 at high temperatures reported so far [1–9] are shown in Fig. 1. Most of the heat capacity data above 1500 K were obtained by means of drop calorimetry; the enthalpy data are obtained, and then heat capacity was calculated by their differentiation with respect to temperature. In Fig. 1, the heat capacity data by Hein et al. [4], Szwarc [6], and Ralph and Hyland [8], were obtained by using the same enthalpy data [4], but they are different from each other, although the remarkable rise of heat capacity above 2000 K is seen in all cases. The former three different heat capacity data [4,6,7] were derived by differentiating different polynomials selected for

* Corresponding author. Tel.: +81-52-789-4682;
fax: 81-52-789-4691.
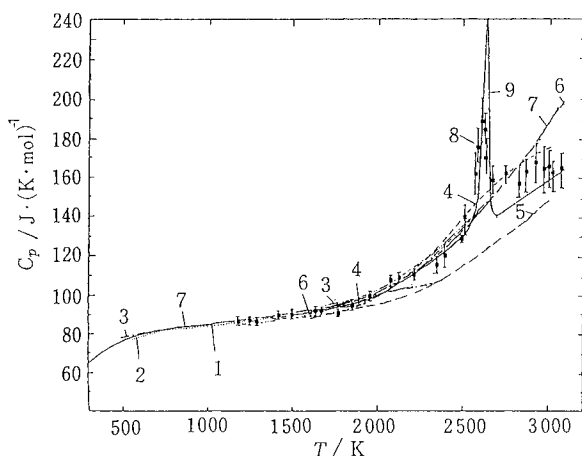*E-mail address*: t-matsui@nucl.nagoya-u.ac.jp (T. Matsui)

Fig. 1. Heat capacity of UO_2 at high temperatures measured by various authors: (1) Grønvold et al. [1], (2) Fredrickson and Chasanov [2], (3) Ogard and Leary [3], (4) Hein et al. [4], (5) Affortit and Marson [5], (6) Szwarc [6], (7) Kerrisk and Clifton [7], (8) Ralph and Hyland [8], (9) Bredig [9].

the same experimental enthalpy increase. On the other hand, the latter data [8] were obtained by applying the quasi-local linear regression method, which is a more acceptable method for the differentiation of the enthalpy data than the normal global regression analysis used for the former three data. This method revealed the presence of a pronounced heat capacity peak at 2610 K. Bredig [9] first pointed out the existence of a lambda-type peak at 2670 K in the heat capacity curve by applying a different polynomial for the same enthalpy data as those used by Hein et al. [4] and Szwarc [6], but excluding only one data point. It

can be stated that (1) the drop method is not for direct heat capacity measurement but for enthalpy determination, (2) the derived values for heat capacity depend on both the selection of the polynomials and the differentiation procedure with respect to temperature, and (3) thermal anomalies such as phase transitions are sometimes overlooked or ignored. Table 1 shows a summary of various methods [10–22] for the precise measurement of heat capacity of mainly ceramic materials, within an error of $\pm 2\%$ at temperatures above 800 K. The high temperature adiabatic calorimetry at temperatures above 1050 K is also not included here since the heat capacity values were measured for metals and alloys within the error of 3–5%. There are four calorimeters, i.e. the direct heating pulse calorimeter [10] previously developed in our laboratory, laser autoclave calorimeter [11–14] developed by the group at Transuranium Institute including one of the present authors, the high temperature differential scanning calorimeter with triple-cells [15], and the high speed cooling calorimeter developed by one of the present authors [16], which are applicable for heat capacity measurements of ceramic materials (not only metallic materials) at high temperatures above 1100 K. Although the direct heating pulse calorimeter was used for the measurements of heat capacity of UO_2 doped with several aliovalent cations [23–28] in our laboratory, a large and long specimen was necessary and temperature was limited up to 1600 K. The high temperature differential calorimeter with triple-cells developed by Asou et al. [15] needs a precise and reproducible calibration between a specimen and a reference sample. The value of this

Table 1
Summary of various methods for precise heat capacity measurements at high temperature above 800 K (excluding the drop method)[a]

Methods	Objective materials		Temperature range/K	Investigators
	Metals	Ceramics		
Adiabatic intermittent heating method (Nernst method)	(a)	(a)	$T \leqq 1050$	Grønvold [17]
Adiabatic scanning method	(a)	(a)	$T \leqq 1000$	Naito et al. [18]
Laser flash method	(a)	(a)	$T \leqq 1000$	Takahashi et al. [19]
Direct heating AC method	(a)	(b)	$T \leqq 3000$	Kraftmakher [20]
Direct heating pulse (intermittent) method	(a)	(a)	$T \leqq 1600$	Naito et al. [10]
High-speed direct heating method	(a)	(b)	$T \geqq 1500$	Cezairliyan [21]
Laser autoclave technique	(a)	(c)	$T \geqq 2000$	Ohse et al. [11–14]
High-temperature differential scanning method (triple-cell)	(a)	(a)	$T \leqq 1500$	Takahashi et al. [15]
High-speed cooling method	(a)	(c)	$T \geqq 2000$	Matsui et al. [16]

[a] (a): Possible, (b): Not suitable, (c): Probably needs several improvements.

calibration factor exceeds 1.0 and increases with increasing temperature above 1000 K according to their results and temperature is limited to be 1500 K.

In this paper, development of two new calorimeters made in our laboratory, i.e. a high speed cooling calorimeter and an advanced-direct heating pulse calorimeter (A-DHPC) are described.

2. Apparatus

2.1. High speed cooling calorimeter

The new dynamic calorimeter, which we call "high speed cooling calorimeter", is schematically shown in Fig. 2 [16]. This calorimeter is assembled of an induction heating furnace, a paraboloidal mirror, and a high speed six-wavelength pyrometer. A small (∼1 mm in diameter) spherical sample is heated from room temperature to any desired high temperature (<2500 K) within 1 s by dropping it through (or suspending it in) a central hole of a tungsten cylindrical pipe in the induction furnace. During drop from the induction furnace, the temperature, T, of the sample decreases with time, t. The cooling rate, dT/dt, and the spectral and total emissivity, ε, of a falling

Fig. 2. Schematic diagram of the high speed cooling calorimeter.

sample are measured simultaneously as a function of time by a six-wavelength pyrometer developed in our laboratory. The optical sensor of the pyrometer is made of a large glass-fiber bundle and is placed at the focal point of a paraboloidal mirror. The basic concept of the lens system of the pyrometer is similar to that reported by the research group at the European Institute for Transuranium Elements [11,29], but the present pyrometer is made compact.

Temperature and emissivity measurements are based on two equations in which one is the Planck and Wien equation

$$J(\lambda, T) = \varepsilon(\lambda, T)C_1\lambda^{-5}\exp(-C_2/\lambda T) \qquad (1)$$

where J is the light flux, λ the wavelength, C_1 and C_2 the radiation constants, and T the temperature. The other is an assumed equation concerning the variation of the spectral emissivity with wavelength expressed.

$$\ln\varepsilon(\lambda, T) = a + b\lambda \qquad (2)$$

where a and b are the function of temperature. The calibration of the pyrometer was made with a standard tungsten ribbon lamp.

The heat capacity (C_p) is determined from the cooling rate given by the following equation which is based on global energy balance:

$$\frac{4}{3}\pi R^3\rho C_p\left(\frac{dT}{dt}\right) = -4\pi R^2(\varepsilon\sigma T^4 + \alpha T) \qquad (3)$$

where R and ρ are the radius and density of the sample, respectively. The energy loss of the spherical sample is given by the loss through radiation (the first term on the right-hand side of Eq. (3), σ is the Stefan–Boltzmann constant) and convection (the second term, α is a constant). Since the loss rate due to convection is negligible in vacuum at high temperature, Eq. (3) is reduced to the following equation:

$$\frac{dT}{dt} = -\frac{3\varepsilon\sigma T^4}{\rho R C_p} \qquad (4)$$

2.2. Advanced direct heating pulse calorimeter

The advanced direct heating pulse calorimeter is schematically shown in Fig. 3 [10]. With this calorimeter, the heat capacity and the electrical conductivity were measured simultaneously. In this calorimeter, the temperature of a sample rod is first increased up to a
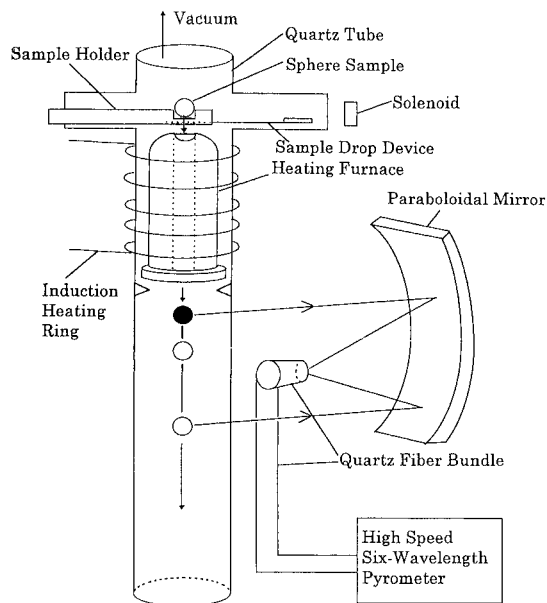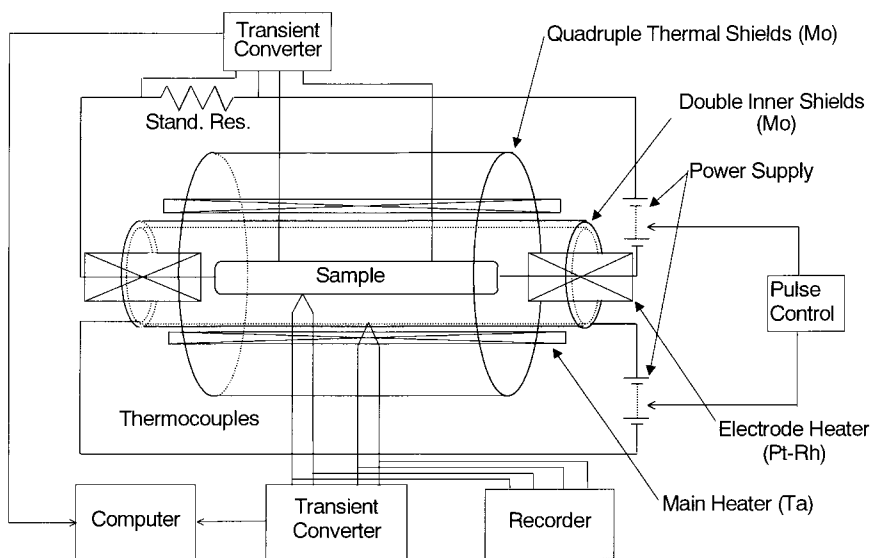
Fig. 3. Schematic diagram of the advanced direct heating pulse calorimeter.

desired temperature by an external heater. Two sub-heaters placed at both ends of samples were used to decrease the temperature gradient in the rod sample and, to decrease heat flow from sample to both ends. After reaching equilibrium (after getting a constant desired temperature), electric power was supplied directly to the sample rod in a short period (usually 0.1–1.2 s) through a regulated d.c. power supply and the temperature rise of the sample (generally 2–4 K) was measured by a Pt/Pt–13%Rh thermocouple of 0.15 mm diameter. In order to reduce the error in heat capacity due to heat leak from the sample at high temperature, a double cylindrical thermal shield made of molybdenum, placed outside the sample, was simultaneously heated electrically using batteries. So as to obtain the same temperature rise as the sample, the adiabatic condition was obtained. The electric potential drop, the current and the temperature rise of the sample rod were simultaneously measured to obtain the heat capacity and the electrical conductivity for a sample.

3. Results and discussion

3.1. High speed cooling calorimeter

As a simulation of measuring cooling curve of a falling sample from an induction furnace, the cooling

curve of the tungsten lamp was measured in the temperature range 2060–2180 K by monitoring its radiance after it had been turned off. The result is shown in Fig. 4. The relationship between temperature and time is linear, indicating the reliability of high speed pyrometer. The maximum temperature (2180 K) measured in this study is higher than that (2100 K) measured in our previous study [16].

As a simulation of a dropped sample, the vertical position of the tungsten lamp (heated at a constant temperature) was changed. The variations of tempera-
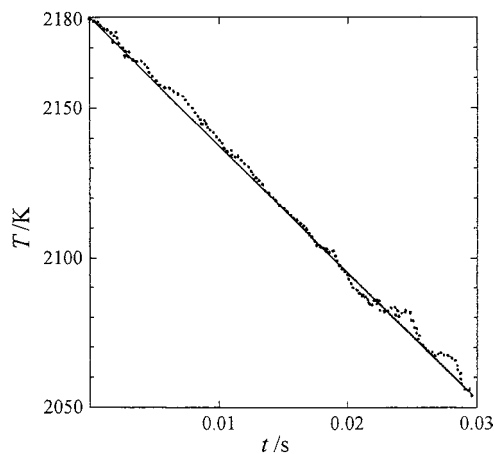

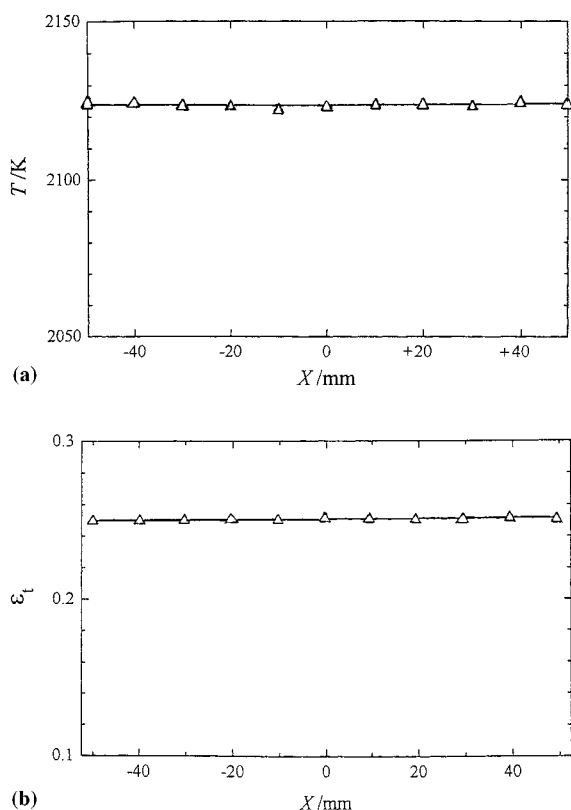Fig. 4. Time dependence of temperature (cooling curve).

Fig. 5. (a) Variation of measured temperature with vertical position of the tungsten lamp; (b) Variation of measured total emissivity with vertical position of the tungsten lamp.

ture and total emissivity with this vertical movement are shown in Fig. 5a and b, respectively. In these figures, the variations of the true temperature and the total emissivity with the vertical movement of ±50 cm are ±1 K and ±1%, respectively, showing the validity of this calorimeter. By the improved geometrical setting of the glass-fiber bundle, the paraboloidal mirror and the tungsten lamp, the variations of temperature and emissivity with vertical movement of the tungsten lamp were drastically decreased in comparison with our previous results (*T*: ±17 K and ε: ±25%) [16].

3.2. Advanced direct heating pulse calorimeter

One of the main difficulties to measure the heat capacity at high temperatures above 1500 K by a direct heating pulse calorimeter is snapping of the

external heating wire. The reasons for the snapping are reaction between Pt–Rh heating wire and Si impurity in the alumina insulator inside which the Pt–Rh heating wire was wound, thinning of the wire by vaporization and partial overheat by recrystallization of the Pt–Rh alloy. We tried to use a tungsten wire as a main heater to increase the measuring temperature. However, the tungsten wire was easily oxidized and snapped soon, since an oxygen partial pressure in a vacuum vessel was not low enough (about 10^{-1} Pa). The high oxygen partial pressure in the vessel was due to: (1) low exhausting rate due to the small inside diameter (low conductance) of the connecting tube between the vacuum vessel and an oil diffusion pump, and (2) large degassing from the thermal insulator made of porous alumina ceramics at high temperatures. Therefore, a new vacuum vessel and a new thermal insulator were designed to achieve low oxygen partial pressure in which the refractory metal is not oxidized. The conductance between the vessel and a vacuum pump was enlarged by about 15 times. The thermal insulator made of four concentric cylindrical molybdenum shields was adopted to decrease the degassing from the thermal insulator. The oxygen partial pressure in this new vessel was finally improved from 10^{-1} to 10^{-5} Pa. Among tungsten, molybdenum and tantalum wires, tantalum wire was selected for the main heater because of its better ductility.

Fig. 6 shows the heat capacity of graphite (70 mm long and 6 mm in diameter) measured by an A-DHPC in the temperature range from 300 to 1750 K. In the
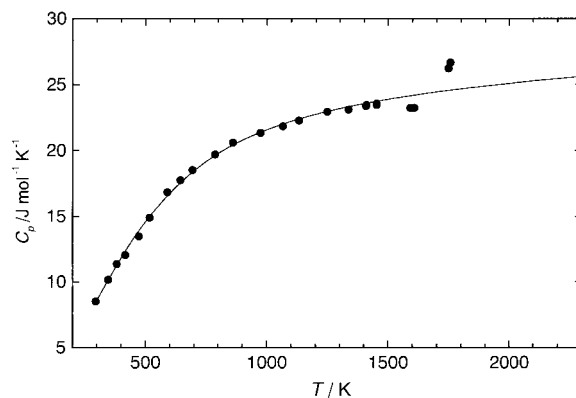

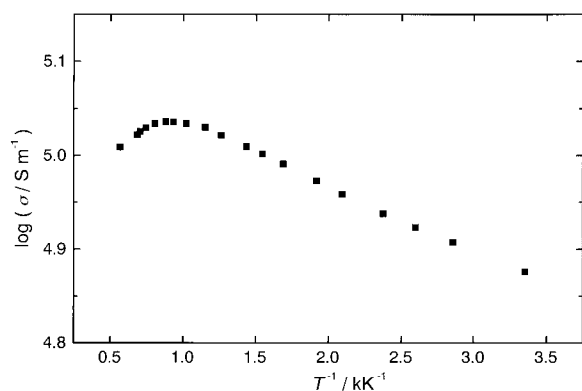Fig. 6. Heat capacity of graphite. (●) This study, (—) Butland and Madison [30].

Fig. 7. Electrical conductivity of graphite. (■) This study.

figure the solid line indicates the previous data compiled by Butland and Madison [30]. It is seen that the heat capacity data measured by A-DHC are in good agreement with their data [30] below 1600 K. A discrepancy from their data was observed at 1750 K. The difference at 1750 K seems to be noise in the signal of thermocouple.

Fig. 7 shows the electrical conductivity of graphite measured simultaneously with the heat capacity by the A-DHPC. The electrical conductivity data of graphite reported by many authors are scattered considerably, due to difference in the preparation and heat treatment of the samples. There are still difficulties to extend the performance of A-DHPC to higher temperatures.

Acknowledgements

References

[1] P. Grønvold, N.J. Kveseth, A. Svean, J. Tichy, J. Chem. Thermodyn. 2 (1970) 665.
[2] D.R. Fredrickson, M.G. Chasanov, J. Chem. Thermodyn. 2 (1970) 623.
[3] A.E. Ogard, J.A. Leary, Proceedings of the Symposium on Thermodynamics of Nuclear Materials, IAEA, Vienna, 1967.
[4] R.A. Hein, P.N. Flagella, J.B. Conway, J. Am. Ceram. Soc. 25 (1968) 99.
[5] C.A. Affortit, J.P. Marcon, Rev. Int. Hautes Temper. Regrat. 7 (1970) 236.
[6] R. Szwarc, J. Phys. Chem. Solids 30 (1969) 705.
[7] J.F. Kerrisk, D.G. Clifton, Nucl. Technol. 16 (1972) 531.
[8] J. Ralph, G.J. Hyland, J. Nucl. Mater. 132 (1985) 76.
[9] M.A. Bredig, Collog. Int. C.N.R 205 (1971) 183.
[10] K. Naito, H. Inaba, M. Ishida, K. Seta, J. Phys. E 12 (1979) 712.
[11] R.W. Ohse, C. Cercignani, A. Frezzotti, J.P. Hiernaut, M. Hoch, G.J. Magill, T. Matsui, P. Werner, J. Metals, 37 TMS-AIME Annual Meeting, Vol. 29, 1985.
[12] R.W. Ohse, Int. J. Thermophys. 11 (1990) 753.
[13] C. Ronchi, J.P. Hiernaut, R. Selfslag, G.J. Hyland, Nucl. Sci. Eng. 113 (1993) 1.
[14] J.P. Hiernaut, G.J. Hyland, C. Ronchi, Int. J. Thermophys. 14 (1993) 259.
[15] M. Asou, T. Yoneoka, T. Terai, Y. Takahashi, in: Proceedings of the 12th IUPAC Conference on Chemical Thermodynamics, Snowbird, USA.
[16] T. Matsui, T. Ishii, R. Sasaki, K. Naito, High Temp.–High Press. 25 (1993) 531.
[17] F. Grønvold, Acta Chem. Scand. 21 (1967) 1695.
[18] K. Naito, H. Inaba, M. Ishida, Y. Sato, H. Arima, J. Phys. E 7 (1974) 464.
[19] Y. Takahashi, J. Nucl. Mater. 51 (1974) 17.
[20] Y.A. Kraftmakher, High Temp.–High Press. 5 (1973) 433.
[21] A. Cezairliyan, M.S. Morse, H.A. Berman, C.W. Beckett, J. Res. Natl. Bur. Stand. A 74 (1970) 65.
[22] C. Ronchi, G.J. Hyland, J. Alloys Comp. 213/214 (1994) 159.
[23] H. Inaba, K. Naito, M. Oguma, J. Nucl. Mater. 149 (1987) 341.
[24] T. Matsui, Y. Arita, K. Naito, J. Radioanal. Nucl. Chem. 143 (1991) 149.
[25] T. Matsui, Y. Arita, K. Naito, Solid State Ionics 49 (1991) 195.
[26] T. Matsui, Y. Arita, K. Naito, J. Nucl. Mater. 188 (1992) 205.
[27] Y. Arita, S. Hamada, T. Matsui, Thermochim. Acta 247 (1994) 225–236.
[28] Y. Arita, S. Hamada, T. Matsui, Thermochim. Acta 253 (1) (1995) 1–9.
[29] J.P. Hiernaut, R. Beukers, M. Hoch, T. Matsui, R.W. Ohse, High Temp.–High Press. 18 (1986) 617.
[30] A.T.D. Butland, R.J. Madison, J. Nucl. Mater. 47 (1973) 45.